

Design Strategies To Improve the Sensitivity of Photoactive Metal Carbonyl Complexes (photoCORMs) to Visible Light and Their Potential as CO-Donors to Biological Targets

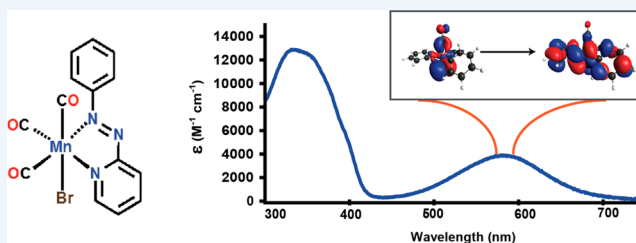
Indranil Chakraborty, Samantha J. Carrington, and Pradip K. Mascharak*

Department of Chemistry and Biochemistry, University of California, Santa Cruz, California 95064, United States

CONSPECTUS: The recent surprising discovery of the beneficial effects of carbon monoxide (CO) in mammalian physiology has drawn attention toward site-specific delivery of CO to biological targets. To avoid difficulties in handling of this noxious gas in hospital settings, researchers have focused their attention on metal carbonyl complexes as CO-releasing molecules (CORMs). Because further control of such CO delivery through light-triggering can be achieved with photoactive metal carbonyl complexes (photoCORMs), we and other groups have attempted to isolate such complexes in the past few years.

Typical metal carbonyl complexes release CO when exposed to UV light, a fact that often deters their use in biological systems. From the very beginning, our effort therefore was directed toward identifying design principles that could lead to photoCORMs that release CO upon illumination with low-power (5–15 mW/cm²) visible and near-IR light. In our work, we have utilized Mn(I), Re(I), and Ru(II) centers (all d⁶ ground state configuration) to ensure overall stability of the carbonyl complexes. We also hypothesized that transfer of electron density from the electron-rich metal centers to π^* MOs of the ligand frame via strong metal-to-ligand charge transfer (MLCT) transitions in the visible/near-IR region would weaken metal–CO back-bonding and promote rapid CO photorelease. This expectation has been realized in a series of carbonyl complexes derived from a variety of designed ligands and smart choice of ligand/coligand combinations.

Several principles have emerged from our systematic approach to the design of principal ligands and the choice of auxiliary ligands (in addition to the number of CO) in synthesizing these photoCORMs. In each case, density functional theory (DFT) and time-dependent DFT (TDDFT) study afforded insight into the dependence of the CO photorelease from a particular photoCORM on the wavelength of light. Results of these theoretical studies indicate that extended conjugation in the principal ligand frames as well as the nature of the donor groups lower the energy of the lowest unoccupied MOs (LUMOs) while auxiliary ligands like PPh₃ and Br[−] modulate the energy of the occupied orbitals depending on their strong σ - or π -donating abilities. As a consequence, the ligand/coligand combination dictates the energy of the MLCT bands of the resulting carbonyl complexes. The rate of CO photorelease can be altered further by proper disposition of the coligands in the coordination sphere to initiate *trans*-effect or alter the extent of π back-bonding in the metal–CO bonds. Addition of more CO ligands blue shift the MLCT bands, while intersystem crossing impedes labilization of metal–CO bonds in several Re(I) and Ru(II) carbonyl complexes. We anticipate that our design principles will provide help in the future design of photoCORMs that could eventually find use in clinical studies.



INTRODUCTION

Although the toxicity of carbon monoxide is well established (often referred to as the silent killer),¹ the salutary effects of this diatomic molecule have only recently been recognized.^{2,3} CO is endogenously produced through the catabolism of heme by the enzyme heme oxygenase (HO).⁴ Surprisingly, at lower concentrations, CO imparts significant anti-inflammatory and antiapoptotic effects in mammalian physiology through various pathways.² CO also provides protection from myocardial infarction⁵ and has been employed during pretreatment in procedures of organ transplantation and preservation.⁶ Despite such beneficial roles of CO in different therapeutic settings, difficulties in handling this toxic gaseous molecule loom as a major concern in CO therapy.⁷ To evade such impediments, researchers have undertaken initiatives to synthesize various

transition metal carbonyl complexes for use as pro-drugs, which eventually deliver CO to biological targets.^{8,9} Many of these carbonyl complexes, commonly known as CORMs (carbon monoxide releasing molecules), undergo solvent-assisted release of CO and thus serve as agents for controlled CO delivery. However, such CORMs often suffer from poor solubility in biological systems, poor stability under aerobic conditions, or shorter half-lives.² These drawbacks call for an alternative trigger for CO release from CORMs in addition to better stability in biological milieu.

To achieve better control of sustainable and site-specific CO delivery, recent efforts in the development of CORMs have

Received: April 28, 2014

Published: July 8, 2014

focused on designed transition metal carbonyl complexes that release CO when triggered with light. These carbonyl complexes, referred to as photoCORMs (photo-induced carbon monoxide releasing molecules), have now emerged as promising CO delivery agents.^{10–12} Long before the concept of CO delivery with metal carbonyl complexes via light illumination, photoactive metal carbonyl complexes raised considerable research interest due to novel electronic properties of their excited states and were explored in a wide variety of photophysical and photochemical research.¹³ Most of the photoCORMs that have been developed in recent years for phototherapy are however based on group 7 and 8 transition metals. A careful scrutiny of the literature also reveals that the majority of the photoCORMs studied so far require *UV light* to trigger CO release.^{11,12} The requirement of a UV light trigger clearly poses a new problem with such photoCORMs because of the detrimental effects of UV light on biological targets. Development of suitably designed photoCORMs that can be activated with *visible light* therefore remains as the major challenge in this area at the present time.

During the past few years, our group has undertaken the task of systematic isolation of designed photoCORMs that can undergo CO release upon exposure with *low power visible light*. In this endeavor, we have focused mainly on group 7 (Mn, Re) and group 8 (Ru) transition metal complexes in their +1 and +2 oxidation states, respectively. These metal centers with low-spin d^6 configuration have been extensively studied due to their rich photophysical and photochemical properties¹³ and thus are ideal candidates for potential photoCORMs. These complexes possess distinct MLCT (metal to ligand charge transfer) transitions that contribute toward metal–CO bond labilization and thereby augment CO release. In this Account, we present the various strategies we have utilized to isolate group 7 and 8 metal-based photoCORMs that can be activated with low power visible light. Unlike other groups, we have employed ligands based on selected design principles that allow isolation of metal carbonyl complexes with strong MLCT bands in the visible region. The correlation between the CO releasing parameters of such complexes and variation in appropriate ligand/coligand combination has been rationalized with DFT (density functional theory) and TDDFT (time-dependent density functional theory) calculations. These studies have provided useful insights toward ligand frames that can indeed shift the low-energy MLCT absorptions toward visible and near-IR regions of the spectrum. We anticipate that our results will also serve as useful guidelines for the future design of novel photoCORMs that could find applications in CO phototherapy.

■ EFFECTS OF CONJUGATION IN THE LIGAND FRAME ON THE ENERGY AND MOLAR ABSORPTIVITY OF THE MLCT BAND IN photoCORMs

In our initial study, we focused on the CO releasing properties of manganese carbonyl complexes derived from polypyridine ligands. The impetus for this early work came from the reports by Schatzschneider¹⁴ and Kunz¹⁵ who studied CO photorelease from $[\text{Mn}(\text{CO})_3(\text{tpa})]^+$ (tpa = tris(pyrazolyl)methane) and $[\text{Mn}(\text{CO})_3(\text{bpma})]^+$ (bpma = bis(pyridylmethyl)amine) complexes, respectively. Although CO release from both compounds required UV light, the utility of such species was evident in successful eradication of cancer cells following CO delivery. Because ligation of CO to metal centers is facilitated

by metal-to-CO back-bonding, transfer of electron density from the metal center to the π^* MO of suitably designed auxiliary ligand (as it happens in a strong MLCT transition) can labilize M–CO bonds. We therefore initiated a systematic investigation of the characteristics of desired ligand frames that could red shift the MLCT band maxima of the carbonyl complexes to the visible region. In the first phase, we synthesized two structurally similar Mn(I) carbonyl complexes, namely, $[\text{Mn}(\text{tpa})(\text{CO})_3]\text{ClO}_4$ (**1**, tpa = tris(pyridyl)amine) and $[\text{Mn}(\text{dpa})(\text{CO})_3]\text{Br}$ (**2**, dpa = *N,N'*-bis(2-pyridylmethyl)amine) to assess the effect on the lowest energy absorption band maximum with increase in number of pyridine rings (Figure 1).¹⁶ Comparison of the

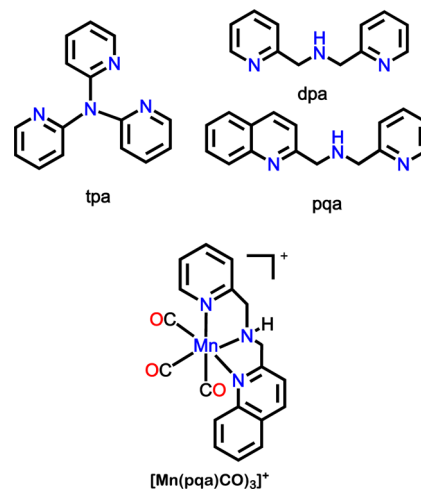


Figure 1. Polypyridine ligands employed in the first-generation photoCORMs and the structure of the cation of **3**.

electronic absorption spectra of **1** ($\lambda_{\text{max}} = 330 \text{ nm}$) and **2** ($\lambda_{\text{max}} = 350 \text{ nm}$) revealed that increase in the number of pyridine N donors in the ligand frame results in a blue shift of the MLCT band. Although ligation of the dpa ligand red shifts the MLCT band, the molar absorptivity of **2** is relatively lower than that of **1** and thus a 20 nm red shift of the photoband in the former is counterweighed by its lower absorption coefficient. When the pyridine moiety of dpa was replaced by a quinoline (more conjugation in the ligand frame), the resulting Mn(I) carbonyl complex $[\text{Mn}(\text{pqa})(\text{CO})_3]\text{ClO}_4$ (**3**, Figure 1, pqa = (2-pyridylmethyl)(2-quinolylmethyl)amine, $\lambda_{\text{max}} = 360 \text{ nm}$) exhibited a further red shift of 10 nm of the MLCT band compared with that of **2**. In addition, the molar absorptivity of the band increased considerably. The CO release from such photoCORMs has been confirmed via myoglobin assay, and all three complexes demonstrate comparable apparent CO release rate (k_{CO}) in MeCN solutions (range: $(8.1\text{--}11.7 \pm 0.1) \times 10^{-2} \text{ s}^{-1}$) upon illumination with low power (5 mW cm^{-2}) UV light.¹⁶ Modest quantum yield values determined at 360 nm (ϕ_{360} , range 0.06–0.09), suggested that slow but sustainable release of CO to specific targets is possible with these photoCORMs. Significant vasorelaxation of rat aorta muscle rings was indeed observed with $10 \mu\text{M}$ of **3** in tissue bath experiment under illumination with ambient light.¹⁶ The photophysical results however indicated that more unsaturation and conjugation in the ligand frame is required for bringing the MLCT band into the visible region.

EFFECTS OF EXTENDED CONJUGATED LIGAND FRAME IN COMBINATION WITH σ -DONOR OR π -ACCEPTOR ANCILLARY LIGANDS ON THE ENERGY OF THE MLCT BAND

In the next stage, we synthesized selected Mn(I) carbonyl complexes derived from a bidentate (pimq, Figure 2) and two

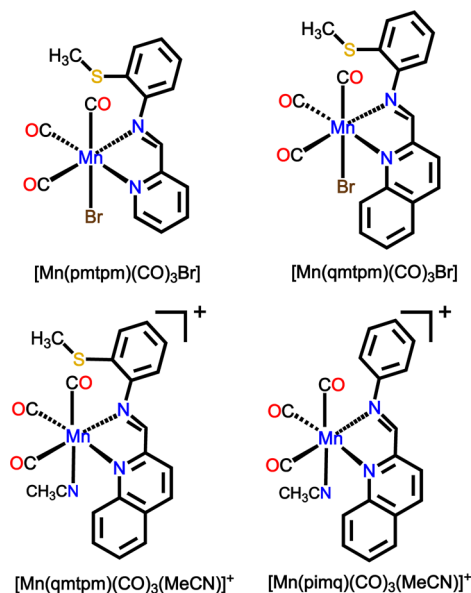


Figure 2. Structures of 4, 6, and the cations of 7 and 8.

potentially tridentate ligands bearing imine functions. A $-SMe$ moiety was added to the tridentate ligand frames to facilitate the CO release through formation of a five-membered chelate ring. Replacement of amine nitrogen (as in dpa ligand) with the imine function is expected to stabilize the lowest unoccupied MO (LUMO) associated with the MLCT transition and thus can lead to a red shift of the photoband toward the visible region. In addition, we utilized Br^- as an ancillary ligand because this strong σ -donor could lower the energy of related MLCT transitions by destabilizing the occupied MOs. The two tridentate N,N,S donor ligands (Figure 2) that we designed are pmtpm (2-pyridyl- N -(2'-methylthiophenyl)methylenimine) and qmtpm (2-quinoline- N -(2'-methylthiophenyl)methylenimine).¹⁷ This choice of the aromatic N -donors was driven by the previous observations that increased conjugation in the ligand frame conferred higher absorptivity as well as resulted in a red shift of the MLCT band in corresponding complexes. With the Mn(I) center, a total of four Mn(I) carbonyl complexes, namely, $[Mn(pmtpm)(CO)_3Br]$ (4), $[Mn(pmtpm)(CO)_3(MeCN)]ClO_4$ (5), $[Mn(qmtpm)(CO)_3Br]$ (6), and $[Mn(qmtpm)(CO)_3(MeCN)]ClO_4$ (7) were isolated, and their structures were verified by X-ray crystallography.¹⁷ In all four complexes, three CO groups are facially disposed and the pmtpm/qmtpm ligand is bound to the metal centers in a bidentate fashion with an uncoordinated $-SMe$ group as an appendage. The equatorial planes in these complexes consist of the two N atoms from the ligands and two CO groups while the third CO and $Br^-/MeCN$ occupy the axial positions (Figure 2).

Electronic absorption spectral studies of the above compounds clearly demonstrated the effects of (a) increased conjugation and (b) σ -donation or π -acceptance by the ancillary ligands. The effect of increased conjugation on the

energy of the MLCT band was evident from a red shift of the absorption band of $[Mn(qmtpm)(CO)_3(MeCN)]ClO_4$ (7, $\lambda_{max} = 435$ nm) compared with that of $[Mn(pmtpm)(CO)_3(MeCN)]ClO_4$ (5, $\lambda_{max} = 390$ nm, Figure 3). Moreover,

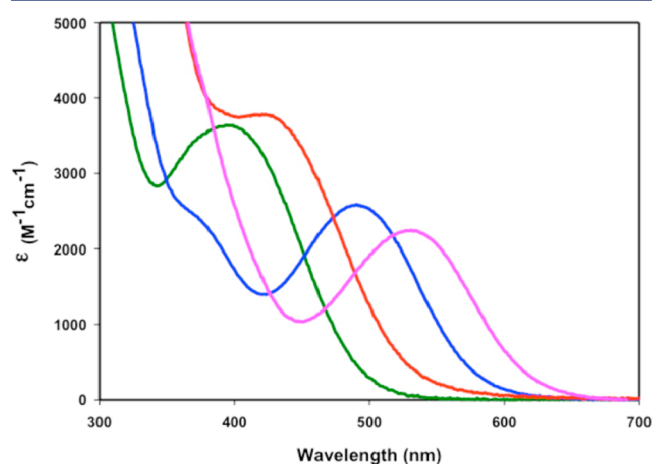


Figure 3. Electronic absorption spectra of $[Mn(pmtpm)(CO)_3Br]$ (4, blue trace), $[Mn(pmtpm)(CO)_3(MeCN)]ClO_4$ (5, green trace), $[Mn(qmtpm)(CO)_3Br]$ (6, pink trace), and $[Mn(qmtpm)(CO)_3(MeCN)]ClO_4$ (7, red trace).

substitution of the MeCN ligand in these complexes with predominantly σ -donating Br^- ligand resulted in further red shift of the absorption maxima ($[Mn(qmtpm)(CO)_3Br]$, 6, $\lambda_{max} = 535$ nm and $[Mn(pmtpm)(CO)_3Br]$, 4, $\lambda_{max} = 500$ nm, Figure 3). As expected, the bromo analogues exhibited CO release upon illumination with low power visible light ($\lambda_{irr} = 509$ nm), which was confirmed by myoglobin assay. Due to differences in solubility, we could not determine the k_{CO} values of all four complexes in the same solvent. However, it is noteworthy to mention that between the two qmtpm-derived carbonyl complexes, the bromo analogue exhibited relatively faster CO photorelease ($(2.6 \pm 0.1) \times 10^{-3} s^{-1}$) compared with that observed with the MeCN-coordinated complex ($(2.0 \pm 0.1) \times 10^{-3} s^{-1}$).¹⁷ Although structural studies revealed that in all complexes the $-SMe$ group remain uncoordinated, it has been realized that inclusion of such a group has significant influence on both k_{CO} and quantum yield values of CO photorelease. A structurally similar Mn(I) carbonyl, namely, $[Mn(pimq)(CO)_3(MeCN)]ClO_4$ (8, pimq = 2-(phenyliminomethyl)quinoline) showed a lower apparent k_{CO} and quantum yield values ($(0.13 \pm 0.1) \times 10^{-3} s^{-1}$ and 0.130 ± 0.005 , respectively) compared with those of the corresponding qmtpm complex 7 ($(2.0 \pm 0.1) \times 10^{-3} s^{-1}$ and 0.208 ± 0.005) respectively.¹⁷

To gain further understanding of the role of extended conjugation and specific donor centers in respective MLCT transitions, we performed DFT and TDDFT calculations on these Mn(I) carbonyl complexes.¹⁷ Analysis of the frontier orbitals corresponding to the lowest energy electronic transition in each case revealed the promotion of electron density from HOMO - 2 with significant $\pi(Mn-CO)$ bonding character to the LUMO (lowest unoccupied molecular orbital) consisting of the imine and the pyridine/quinoline π^* antibonding orbitals. Comparison of the relative energies of HOMO - 2 and LUMO in two bromo analogues, 4 and 6, demonstrated the effect of extended conjugation in the ligand frame (change from pyridine to quinoline) on the HOMO - 2

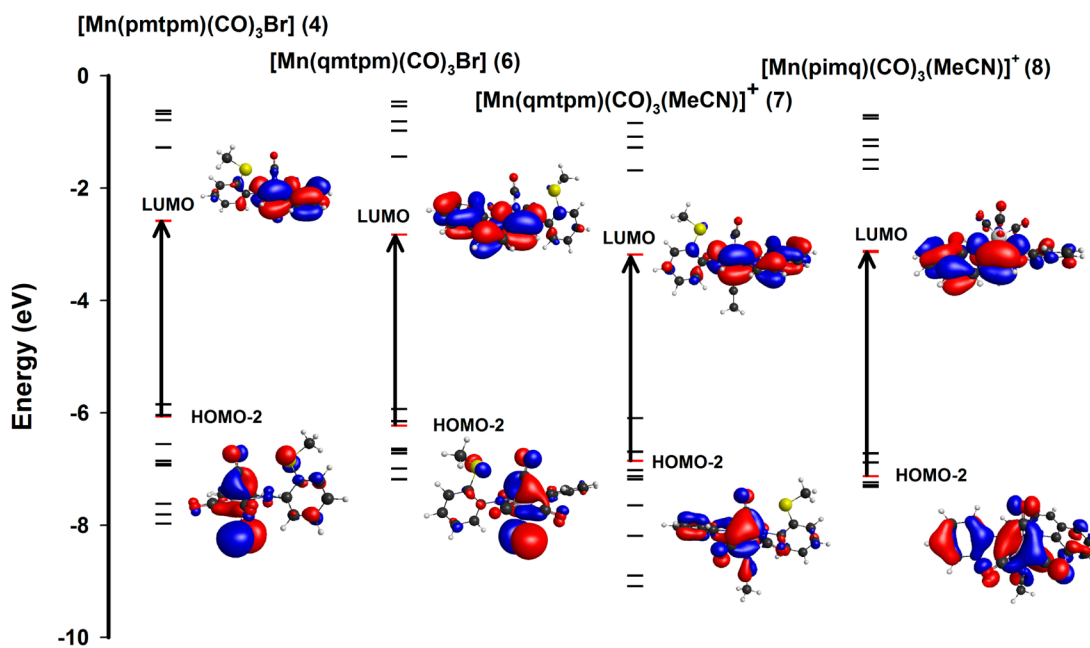


Figure 4. Calculated HOMO/LUMO energy diagram of complexes 4, 6, 7, and 8 (from left to right). The most prominent MOs involved with transitions under the low-energy band and their diagrams are shown. Transitions discussed in the text are shown (the orbitals in TDDFT calculations are also shown).

→ LUMO transition. In the qmtpm complex, the LUMO is significantly stabilized compared with that in the pmtpm complex (Figure 4). As a consequence, the energy difference between HOMO – 2 and LUMO decreases noticeably from the pmtpm to qmtpm complex, which is in accordance with the experimentally observed red shift of the MLCT band maximum from 500 to 535 nm. Assessment of the frontier orbitals for $[\text{Mn}(\text{qmtpm})(\text{CO})_3\text{Br}]$ (6) and $[\text{Mn}(\text{qmtpm})(\text{CO})_3(\text{MeCN})]\text{ClO}_4$ (7) revealed the effect of the ancillary ligand (Br^- vs MeCN) on the relative energies of HOMO – 2 and LUMO in such species. In the case of the bromo analogues, the σ -donating Br^- ligand raised the HOMO – 2 level at significantly higher energy compared with the HOMO – 2 level of the MeCN-coordinated species and resulted in red shift of the HOMO – 2 → LUMO transition as noted experimentally (λ_{max} for 7 = 435 nm, λ_{max} for 6 = 535 nm). Finally, to determine the role of the –SMe appendage of the qmtpm and pmtpm ligands on the energy of the HOMO – 2 → LUMO transition, we compared the energy of the frontier orbitals associated with such transition in 7 with that in another Mn(I) carbonyl 8 derived from a very similar ligand frame, pimq, without the –SMe appendage. Although the energies of the LUMOs of 7 and 8 were comparable, the slightly elevated HOMO – 2 of 7 resulted in a red shift of the photoband (λ_{max} for 7 = 435 nm, for 8 = 430 nm). Taken together, these results indicated that both extended conjugation in the ligand frame and a σ -donating ancillary ligand (such as Br^-) contribute considerably toward red shift of the MLCT band of these carbonyl complexes. Replacement of Br^- with a moderately π -accepting ligand such as MeCN however lowers the energy of HOMO – 2 and causes significant blue shift of the MLCT band. For example, 7 exhibits its MLCT band with λ_{max} at 435 nm compared with 535 nm for 6. As a result, among the Mn(I) complexes 4–8, only 4 and 6 rapidly photorelease CO upon exposure to low power (10–15 mW/cm²) visible light.

■ EFFECT OF THE NUMBER OF CO LIGANDS ON THE ENERGY OF THE MLCT BAND

Poor affinity of the Mn(I) center toward the thioether group did not allow the N,N,S ligands (pmtpm and qmtpm) to coordinate as tridentate ligands in 4–7 (Figure 2). A close survey of the literature revealed that electron-rich group 7 metals ($M = \text{Mn}, \text{Tc}, \text{and Re}$) in +1 oxidation state (d^6 configuration) prefer three CO ligands in facial disposition and afford complexes with the *fac*- $[\text{M}(\text{CO})_3]$ moiety. In comparison, Ru(II) centers (also d^6 configuration) give rise to a variety of carbonyl complexes with the $[\text{Ru}(\text{CO})_2]$ fragment.¹³ Apparently, the Ru(II) centers in these complexes can back-bond with only two CO ligands. We therefore attempted to synthesize Ru(II) complexes of the qmtpm ligand with two (and possibly one) CO ligand and assess the effect of the number of CO ligands in the overall CO photolability.

Reaction of $[\text{RuCl}_2(\text{CO})_3]_2$ (CORM-2) with qmtpm in MeOH afforded $[\text{Ru}(\text{qmtpm})(\text{CO})_2\text{Cl}]\text{ClO}_4$ (9) in which the qmtpm ligand is coordinated to the metal center in a tridentate fashion. The high affinity of the Ru(II) center toward S donors did result in the expected tridentate coordination of the qmtpm ligand in 9 (Figure 5). The planar qmtpm ligand occupies the equatorial plane (along with one CO) and the two CO ligands are *cis* to each other.¹⁸ An analogous qmtpm complex with one

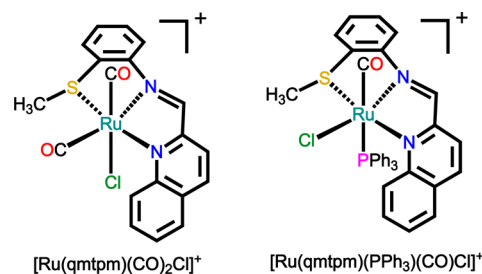


Figure 5. Structures of the cations of 9 and 10.

CO, namely, $[\text{Ru}(\text{qmtpm})(\text{PPh}_3)(\text{CO})\text{Cl}]\text{BF}_4$ (**10**), and one solvent-bound species, $[\text{Ru}(\text{qmtpm})(\text{PPh}_3)(\text{MeCN})_2](\text{ClO}_4)_2$ (**11**), were also synthesized from $[\text{Ru}(\text{qmtpm})(\text{PPh}_3)\text{Cl}_2]$ as the starting material. The electronic absorption spectra of **9–11** clearly demonstrated the effect of (a) the number of CO ligands and (b) replacement of CO groups with other π -acceptor ligands on the energy of the MLCT bands in these complexes.¹⁸

In acetonitrile, the MLCT absorption of $[\text{Ru}(\text{qmtpm})(\text{CO})_2\text{Cl}]\text{ClO}_4$ (**9**) appeared as a shoulder with maximum at 405 nm, and replacement of a CO ligand with PPh_3 resulted in a red shift of this band in the case of $[\text{Ru}(\text{qmtpm})(\text{CO})(\text{PPh}_3)\text{Cl}]\text{BF}_4$ (**10**, $\lambda_{\text{max}} = 465$ nm). Again, replacement of a Cl^- (a σ donor) and a CO (a strong π -acceptor) in **10** with two MeCN ligands (moderate π -acceptor) resulted a red shift of the MLCT band ($\lambda_{\text{max}} = 495$ nm) in $[\text{Ru}(\text{qmtpm})(\text{PPh}_3)(\text{MeCN})_2](\text{ClO}_4)_2$ (**11**). These findings indicate that changes in the number of π -acceptor ligands of varied strengths around the central metal in conjunction with σ -donor ligands (like Cl^-) can readily tune the energy of the photoband (MLCT band). Interestingly, **10** exhibited CO release upon illumination with low power ($15 \text{ mW}/\text{cm}^2$) visible light, while **9** (with two CO ligands) released CO only upon exposure to UV-light ($7 \text{ mW}/\text{cm}^2$). For example, in acetonitrile, **10** rapidly releases CO ($k_{\text{CO}} = (10.5 \pm 0.1) \times 10^{-3} \text{ s}^{-1}$) under visible light with ≥ 440 nm cutoff filter, while **9** releases CO ($k_{\text{CO}} = (3.6 \pm 0.1) \times 10^{-3} \text{ s}^{-1}$) only when exposed to UV light with λ_{max} centered at 310 nm.¹⁸

The fine-tuning of the MLCT bands in **9–11** complexes can be rationalized on the basis of the results of DFT studies.¹⁸ Analysis of the frontier orbitals involved in the low energy transitions indicated that for the two carbonyl complexes **9** and **10**, the two highest occupied orbitals with Ru-ligand bonding character were HOMO – 2/HOMO – 3 and HOMO – 1/HOMO – 3 respectively. The HOMO – 2 and HOMO – 3 MOs of **9** were found to be very closely spaced and comprised of $\pi(\text{Ru}-\text{CO})$ and $\pi(\text{Ru}-\text{Cl})$ bonding characters (Figure 6). In **10**, the HOMO – 1 was composed of mostly $\pi(\text{Ru}-\text{CO})$ bonding character with a minor $\pi(\text{Ru}-\text{PPh}_3)$ bonding contribution, while strong $\pi(\text{Ru}-\text{PPh}_3)$ bonding interactions contributed primarily to HOMO – 3. The LUMO in both cases was mostly composed of π^* antibonding orbitals from the quinoline moiety and the imine function. A close look at Figure 6 reveals that the highest occupied MO in the dicarbonyl complex **9** (HOMO – 2) is of lower energy than that (HOMO – 1) in the monocarbonyl complex **10**. This is anticipated because CO is a superior π -acceptor and thereby stabilizes the HOMO – 2 in **9**. As a consequence, the absorption maximum of the MLCT band of **9** ($\lambda_{\text{max}} = 405$ nm) is red-shifted to 460 nm in case of **10**. The disposition of the Cl^- ligand *trans* to the axial CO group in **9** promotes strong back-bonding between Ru and CO. This was also evident from the $\pi(\text{Ru}-\text{Cl})$ contributions in the HOMO – 2 and HOMO – 3 MOs of **9**. In contrast, Ru–CO labilization in **10** was facilitated by competition between the axial CO and PPh_3 ligand *trans* to it. Furthermore, replacement of one CO ligand in the dicarbonyl complex with one PPh_3 group destabilized both HOMO – 1 and HOMO – 3 MOs of **10** (Figure 6) resulting in shift of the MLCT band to lower energy. Both these factors contributed toward CO photorelease observed for **10** upon exposure to visible light. Results of this study pointed to an interesting fact: increasing the number of CO's causes shift of the photoband into the UV region (most carbonyl complexes with three to five CO's are pale yellow to orange in color) and hence synthetic

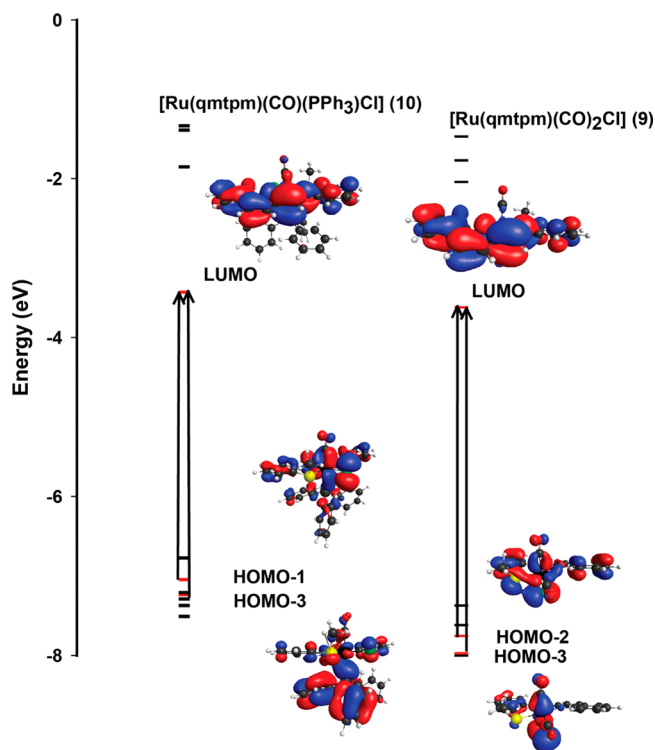


Figure 6. Calculated HOMO/LUMO energy diagram of **9** and **10** (from right to left). The most prominent MOs involved with transitions under the low-energy band and their diagrams are shown.

attempts to isolate photoCORMs with sensitivity to visible light should include *fewer* CO ligands in their coordination sphere.

■ AZO-IMINE VERSUS α' -DIIMINE FUNCTIONALITY

To extend our strategic design to develop photoCORMs that could be triggered with visible/near-IR light for CO release, we have recently focused on ligand frames with the *azo-imine* function. In our initial attempt, the ligand 2-phenylazopyridine (azpy) was employed as bidentate *N,N*-donor ligand to isolate low spin ruthenium carbonyls.¹⁹ The superior π -acceptor character of this ligand compared with diimine type ligands (as employed previously)¹³ arises from the low-lying π^* MO of the $-\text{N}=\text{N}-$ moiety. We hypothesized that low energy MLCT transitions in metal carbonyls derived from azpy would accentuate Ru–CO labilization under visible light. Reaction of $[\text{Ru}_2\text{Cl}_2(\text{CO})_3]_2$ with azpy in MeOH furnished two isomers, namely, *cis*- and *trans*- $[\text{Ru}(\text{azpy})(\text{CO})_2\text{Cl}_2]$ (**12**, **13**). X-ray structural studies confirmed that in both isomers the two CO groups are in *cis* disposition and the relative placement of two Cl^- ligands gave rise to the *cis* and *trans* isomers in $[\text{Ru}(\text{azpy})(\text{CO})_2\text{Cl}_2]$ (Figure 7).¹⁹ The electronic absorption spectra of these low-spin d^6 ground state complexes exhibited two strong bands centered at 360 and 500 nm. The 500 nm band was assigned to a MLCT transition much like that observed in structurally related $[\text{Ru}(\text{bpy})(\text{CO})_2\text{Cl}_2]$ (bpy = bipyridine) complex.²⁰ However, the MLCT transition appeared at relatively lower energy compared with other ruthenium carbonyls incorporating diimine type ligands.¹³ This is most probably due to the stabilization of the LUMOs in **12** and **13**. The two isomers exhibited CO release upon exposure to low power UV light ($5 \text{ mW}/\text{cm}^2$, $\lambda \geq 325$ nm) as confirmed by myoglobin assay. Interestingly, the value of k_{CO} in

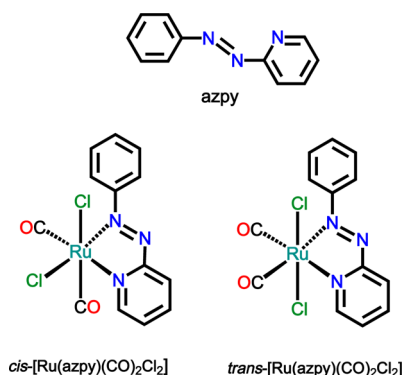


Figure 7. Structures of azpy, 12, and 13.

dichloromethane solution for the *trans* isomer 13 ($(9.16 \pm 0.01) \times 10^{-3}$) was significantly faster than that of the *cis* complex 12 ($(3.17 \pm 0.01) \times 10^{-3} \text{ s}^{-1}$).¹⁹ A close look at the structures of the two carbonyl complexes revealed that in 13, relative disposition of the two Cl[−] ligands brings one CO ligand *trans* to the N atom of the azo function. As a consequence, the back-bonding competition between CO and azo-nitrogen for the same metal orbital in the *trans* isomer enhances the labilization of the Ru–CO bond. It is noteworthy to mention that despite lower molar absorptivity, 13 (the *trans* isomer) exhibited faster CO release compared with 12 (the *cis* isomer). The strong π -acidity of the azo function in the former leads to preferential labilization of the CO ligand *trans* to it and thus overcompensates the effect of lower extent of light absorption.

■ EFFECT OF FIRST ROW VERSUS THIRD ROW TRANSITION METALS IN CO PHOTORELEASE

The effect of pronounced π -acidity of the azo–imine ligand azpy on the k_{CO} values of 12 and 13 encouraged us to isolate Mn(I) and Re(I) carbonyls with the same ligand. The inherent stability of the d⁶ Re(I) carbonyl complexes is often emphasized for their application in various biological studies. Recently, Ford and co-workers have reported a Re(I) based water-soluble photoCORM, namely, [Re(bpy)(thp)(CO)₃] (thp = tris(hydroxymethyl)phosphine) that exhibits minimal toxicity toward human prostatic carcinoma (PCC) cells.²¹ However, CO release from this photoCORM has only been achieved with the aid of UV light, a clear disadvantage for employing such a complex therapeutically.

Reaction of [MnBr(CO)₅] and [ReBr(CO)₅] with azpy in equimolar ratio afforded the *fac*-[Mn(azpy)(CO)₃Br] (14)^{22,23} and *fac*-[Re(azpy)(CO)₃Br] (15)²³ (Figure 8), respectively. In addition, *fac*-[Mn(azpy)(CO)₃(PPh₃)]ClO₄ (16) and *fac*-[Re(azpy)(CO)₃(PPh₃)]ClO₄ (17, Figure 8) were synthesized through replacement of the Br[−] ligand with PPh₃. In all these structurally characterized complexes, the three COs are facially disposed and the azpy ligand binds the metal centers in a bidentate fashion. The uniform lengthening of the N=N bond of the azo moiety indicated significant metal → azo back-bonding interactions in these complexes. The electronic absorption spectra of these complexes revealed the effect of Br[−] (a strong σ -donor) versus PPh₃ (a good π -acceptor) coligands on their MLCT bands. More importantly, our studies unveiled the role of the central metal (manganese versus rhenium) on the photosensitivity of these carbonyl complexes toward lights of different wavelengths. For example, replacement of Br[−] by PPh₃ ligand caused a significant blue shift of the

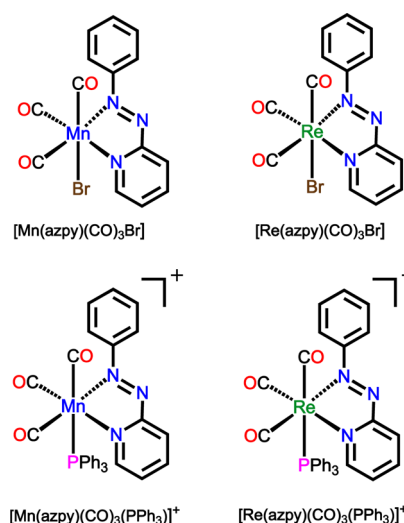


Figure 8. Structures of 14, 15, and the cations of 16 and 17.

λ_{max} of the low-energy band of 14 (586 nm) to 520 nm in case of 16.²² Further, both bromide complexes 14 and 15 exhibited strong absorption in the visible region centered at 586 and 530 nm, respectively (Figure 9). This is noteworthy because the

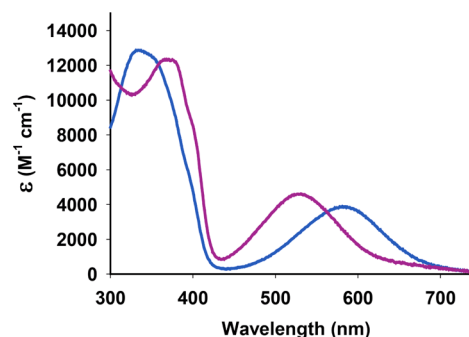


Figure 9. Electronic absorption spectra of 14 (blue trace) and 15 (purple trace) in dichloromethane.

structurally similar bipyridine (bpy) analogues, namely, *fac*-[Mn(bpy)(CO)₃Br] and *fac*-[Re(bpy)(CO)₃Br], display the lowest energy absorption bands at 430 and 400 nm, respectively, under similar experimental conditions.²⁴ It is therefore evident that compared with diimine ligands like bpy, a superior π -accepting azo–imine ligand (such as azpy) contributes more toward significant red shift of the low energy bands in the corresponding complexes.

Among the complexes of Figure 8, only 14 showed rapid CO release when illuminated with low power (10–15 mW/cm²) visible light.²² The k_{CO} value for this complex in dichloromethane solution was found to be $(3.7 \pm 0.1) \times 10^{-1} \text{ s}^{-1}$. The k_{CO} value dropped slightly when the photolysis was carried out with $\lambda \geq 520 \text{ nm}$ cutoff filter. High k_{CO} ($(1.87 \pm 0.1) \times 10^{-1} \text{ s}^{-1}$) and quantum yield value at 550 nm ($\phi_{550} = 0.48 \pm 0.01$) were also noted in acetonitrile. Substantial solubility in acetonitrile–water (20:80 v/v) allowed us to employ 14 in biological studies. This manganese photoCORM was found to be very efficient in eradicating HeLa and human breast cancer MDA-MD-231 cells under the control of visible light.²² A dose-dependent extinction of these two cells and about 50% reduction in viability was observed with a maximum of 75

μM **14** and 10 min of light exposure in both cases. These effects were comparable to that with 10 μM of 5-fluorouracil.

Surprisingly, despite the presence of a strong MLCT band at 530 nm (Figure 9), **15** showed no photoactivity under visible light.²³ This complex exhibited CO release only upon exposure with low power UV light (centered at 305 nm, 5 mW/cm²). Moreover, the k_{CO} value of **15** ($(4.17 \pm 0.01) \times 10^{-3} \text{ s}^{-1}$) was found to be significantly lower in dichloromethane compared with that of **14**. The trend in light sensitivity and the k_{CO} values was consistent in the corresponding PPh₃ complexes. For example, the k_{CO} values of **16** and **17** were found to be $(2.56 \pm 0.01) \times 10^{-1}$ and $(3.50 \pm 0.01) \times 10^{-3} \text{ s}^{-1}$, respectively, in dichloromethane.

Analysis of the frontier orbitals of **14** (DFT studies) suggested that the absorption at 586 nm has its origin in a HOMO - 1 \rightarrow LUMO transition (Figure 10). The HOMO -

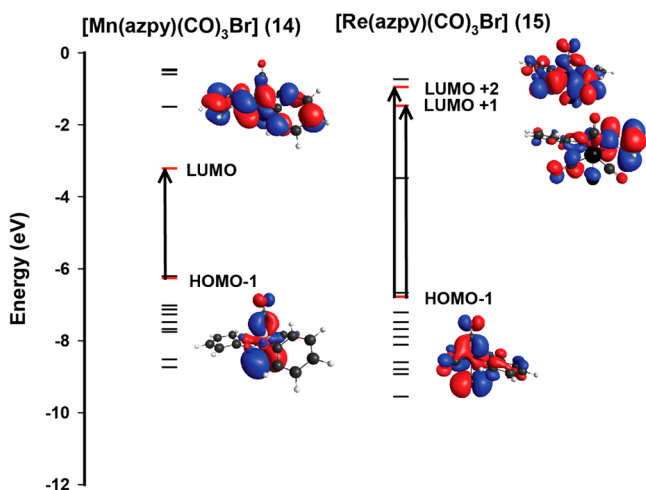


Figure 10. Calculated energy diagram of **14** and **15**. The most prominent MOs involved with transitions under the band associated with CO release and their compositions are shown.

1 of **14** was predominantly of $\pi(\text{Mn}-\text{CO})$ and $p(\text{Br})$ bonding character, while the LUMO comprised the $\text{azpy}-\pi^*$ antibonding orbitals. Due to almost equal participation of $\pi(\text{Mn}-\text{CO})$ and $p(\text{Br})$ orbitals to HOMO - 1, the above transition can be visualized as a MLCT(metal $\rightarrow \pi^*$ ligand)/XLCT(halide $\rightarrow \pi^*$ ligand) combination. Upon illumination, the electron density shifted to LUMO with significant reduction of $p(\text{Br})$ electron density. This indicated that in **14**, both MLCT and XLCT transitions contribute toward the Mn-CO bond labilization and results in a rapid CO release upon exposure to visible light. The composition of the frontier orbitals of **15** related to its 530 nm absorption band was found to be very similar (HOMO - 1 \rightarrow LUMO). However, in this case, illumination of visible light did not trigger any CO release. Only the absorption around 300 nm related to HOMO - 1 \rightarrow LUMO + 1/LUMO + 2 transitions resulted in CO release. The LUMO + 1 was mostly of $\text{azpy}-\pi^*$ antibonding character, while the LUMO + 2 had a major contribution from the $\pi^*(\text{Re}-\text{CO})$ antibonding MO.

Despite the very similar nature of the MLCT/XLCT bands for both the bromo complexes **14** and **15**, the higher propensity of spin-orbit coupling (heavy-atom effect) leads to facile intersystem crossing to ³MLCT excited state in the rhenium carbonyl complex **15**. This state was previously found to be nondissociative in terms of metal-CO bond and to dissipate the energy in the form of other nonradiative processes.^{24,25}

Although the intersystem crossing is still relevant in the excited state of higher energy transition (UV-excitation), the potential energy surface of high-energy ¹MLCT is somewhat more dissociative, which in general leads to Re-CO bond labilization. This is due to the strongly avoided crossing with high-lying ¹LF or ¹MC states along the reaction coordinate²⁶ that consequently results in a minor CO photorelease consistent with experimental findings ($k_{\text{CO}} = (4.17 \pm 0.01) \times 10^{-3} \text{ s}^{-1}$). Indeed, results of previous photochemical ligand substitution studies on Re(I) carbonyls derived from diimine ligands show that CO loss in the majority of the cases can be initiated only with UV-light.²⁷ The results of comparative studies on **14** and **15** thus clearly indicate that the presence of a strong MLCT band in the visible region may not be a sufficient prerequisite for activation of a photoCORM by visible light. Along same line, despite a strong MLCT band around 500 nm, the Ru(II) carbonyl complexes **12** and **13** also fail to release CO upon illumination with visible light.

Comparison of the absorption parameters of **14** and **16** demonstrated the effect of soft auxiliary ligands (like Br⁻) on CO photorelease. In dichloromethane, **14** exhibited faster CO release than **16** ($(3.7 \pm 0.1) \times 10^{-1}$ and $(2.56 \pm 0.01) \times 10^{-1} \text{ s}^{-1}$ respectively) upon exposure to visible light. This was in contrast to general observations where the inclusion of a PPh₃ group has been shown to augment the CO release through weakening of the metal-CO bond *trans* to it.²¹ Analysis of frontier orbitals of **16** revealed that the 520 nm band is related to HOMO - 4 \rightarrow LUMO transition. Here the HOMO - 4 consisted of $\pi(\text{Mn}-\text{CO})$ and $\pi(\text{PPh}_3)$ bonding MOs, and the LUMO had major contribution from $\text{azpy}-\pi^*$ antibonding orbitals. The MLCT in **16** shifted electron density mostly from the $\pi(\text{PPh}_3)$ bonding MO rather than from $\pi(\text{Mn}-\text{CO})$ and as a consequence the Mn-CO bond suffered minor weakening. These findings suggest that soft donor ligands such as Br⁻ can aid in causing a red shift as well as promote CO release through MLCT/XLCT transitions.

CONCLUDING REMARKS

The therapeutic effects of CO have so far been established in animal models, and one blind, randomized, placebo-controlled phase I human trial has been completed at this time.² The use of CORMs however has been accepted as a controlled CO delivery mode^{2,8} and the use of light as a trigger to initiate such delivery appears to be a very desirable goal. In this regard, attempts should be directed toward photoCORMs that can be activated by visible and near-IR light simply because of the detrimental effects of UV light on biological targets. In our work, we have focused on the design principles that would afford such carbonyl complexes and so far we been able to isolate photoCORMs that can be activated by visible light. More toxicity studies and the side effects arising from the photoproducts are however required before such complexes could enter into clinical trials. The side effects of the photoproducts could be curtailed by incorporating suitable photoCORMs into porous biocompatible particles that retain such products within the matrix. We have recently reported 50 nm Al-MCM-41 nanoparticles with $[\text{Mn}(\text{CO})_3(\text{pqa})]\text{ClO}_4$ (**3**) incorporated within its mesoporous structure and demonstrated their utility in vasorelaxation of rat aorta muscle rings through light-induced CO delivery.²⁸ Schatzschneider and co-workers have utilized silica nanoparticles as photoCORM carriers²⁹ and also functionalized photoCORMs for further attachments of peptides for site-specific delivery.³⁰ It is quite

reasonable to expect that more studies along these lines will eventually yield photoCORMs that can be employed for safe delivery of salutary doses of CO to biological targets under the control of light.

AUTHOR INFORMATION

Corresponding Author

*E-mail: pradip@ucsc.edu.

Funding

Financial support from NSF Grants CHE-0957251 and DMR-1105296 is gratefully acknowledged.

Notes

The authors declare no competing financial interest.

Biographies

Indranil Chakraborty received his Ph. D. from Indian Association for the Cultivation of Science in Calcutta, India, under the guidance of Prof. A. Chakravorty in 2003. He did his postdoctoral research at the University of Puerto Rico and University of Texas, El Paso, before he joined the research group of Prof. Pradip Mascharak at University of California, Santa Cruz, as a research scientist. At present, he is working in the area of development of novel photoCORMs for CO delivery to biological targets.

Samantha Carrington received her B.S. in chemistry from the Sonoma State University in 2011. She then joined the graduate program at the University of California, Santa Cruz, and at this time is working in the area of isolation of designed photoCORMs suitable for CO delivery under the control of visible light. She also performs DFT and TDDFT calculations to guide the design processes in such pursuit.

Pradip Mascharak, Distinguished Professor of Chemistry and Biochemistry at the University of California, Santa Cruz, is a bioinorganic chemist. He received his Ph.D. from the Indian Institute of Technology at Kanpur, India, in 1978 and did his postdoctoral work with Prof. Richard Holm first at Stanford University and then at Harvard University. He also worked as a research associate with Prof. Steve Lippard at Massachusetts Institute of Technology for two years before he joined the Department of Chemistry and Biochemistry in 1984. His research interests span a wide range of areas including modeling the active sites of metalloenzymes, drug–receptor interactions, delivery of small signaling molecules (such as NO and CO) to biological targets, and design of biomaterials for drug delivery.

REFERENCES

- (1) Chance, B.; Erecinska, M.; Wagner, M. Mitochondrial Responses to Carbon Monoxide Toxicity. *Ann. N.Y. Acad. Sci.* **1970**, *174*, 193–204.
- (2) Motterlini, R.; Otterbein, L. The Therapeutic Potential of Carbon Monoxide. *Nat. Rev. Drug Discovery* **2010**, *9*, 728–743.
- (3) Heinemann, S. H.; Hoshi, T.; Westerhausen, M.; Schiller, A. Carbon Monoxide – Physiology, Detection and Controlled Release. *Chem. Commun.* **2014**, *50*, 3644–3660.
- (4) Kikuchi, G.; Yoshida, T.; Noguchi, M. Heme Oxygenase and Heme Degradation. *Biochem. Biophys. Res. Commun.* **2005**, *338*, 558–567.
- (5) Stein, A. B.; Bolli, R.; Dawn, B.; Sanganalath, S. K.; Zhu, Y.; Wang, O. L.; Guo, Y.; Motterlini, R.; Xuan, Y. T. Carbon Monoxide Induces a Late Preconditioning-mimetic Cardioprotective and Antiapoptotic Milieu in the Myocardium. *J. Mol. Cell. Cardiol.* **2012**, *52*, 228–236.
- (6) Kohmoto, J.; Nakao, A.; Stolz, D. B.; Kaizu, T.; Tsung, A.; Ikeda, A.; Shimizu, H.; Takahashi, T.; Tomiyama, K.; Sugimoto, R.; Choi, A. M. K.; Billiar, T. R.; Murase, N.; McCurry, K. R. Carbon Monoxide

Protects Rat Lung Transplants From Ischemia-Reperfusion Injury via a Mechanism Involving p38 MAPK Pathway. *Am. J. Transplant.* **2007**, *7*, 2279–2290.

(7) Alberto, R.; Motterlini, R. Chemistry and Biological Activities of CO-releasing Molecules (CORMs) and Transition Metal Complexes. *Dalton. Trans.* **2007**, 1651–1660.

(8) Romão, C. C.; Blättler, W. A.; Seixas, J. D.; Bernardes, G. J. L. Developing Drug Molecules for Therapy with Carbon Monoxide. *Chem. Soc. Rev.* **2012**, *41*, 3571–3583.

(9) Johnson, T. R.; Mann, B. E.; Clark, J. E.; Foresti, R.; Green, C. J.; Motterlini, R. Metal Carbonyls: A New Class of Pharmaceuticals? *Angew. Chem., Int. Ed.* **2003**, *42*, 3722–3729.

(10) Gonzalez, M. A.; Mascharak, P. K. Photoactive Metal Carbonyl Complexes as Potential Agents for Targeted CO Delivery. *J. Inorg. Biochem.* **2013**, *133*, 127–135.

(11) Rimmer, R. D.; Pierrri, A. E.; Ford, P. C. Photochemically Activated Carbon Monoxide Release For Biological Targets. Toward Developing Air-stable photoCORMs Labilized by Visible Light. *Coord. Chem. Rev.* **2012**, *256*, 1509–1519.

(12) Schatzschneider, U. photoCORMs: Light-Triggered Release of Carbon Monoxide from the Coordination Sphere of Transition Metal Complexes for Biological Applications. *Inorg. Chim. Acta* **2011**, *374*, 19–23.

(13) Stufkens, D. J.; Vlcek, A., Jr. Ligand-Dependent Excited State Behaviour of Re(I) and Ru(II) Carbonyl-diimine Complexes. *Coord. Chem. Rev.* **1998**, *177*, 127–179.

(14) Niesel, J.; Pinto, A.; N'Dongo, H. W. P.; Merz, K.; Ott, I.; Gust, R.; Schatzschneider, U. Photoinduced CO release, Cellular Uptake and Cytotoxicity of a tris(pyrazolyl)methane (tpm) Manganese Tricarbonyl Complex. *Chem. Commun.* **2008**, 1798–1800.

(15) Brueckmann, N. E.; Wahl, M.; Reiss, G. J.; Kohns, M.; Watjen, W.; Kunz, P. C. Polymer Conjugates of Photoinducible CO-Releasing Molecules. *Eur. J. Inorg. Chem.* **2011**, *29*, 4571–4577.

(16) Gonzalez, M. A.; Yim, M. A.; Cheng, S.; Moyes, A.; Hobbs, A. J.; Mascharak, P. K. Manganese Carbonyls Bearing Tripodal Polypyridine Ligands as Photoactive Carbon Monoxide-Releasing Molecules. *Inorg. Chem.* **2012**, *51*, 601–608.

(17) Gonzalez, M. A.; Carrington, S. J.; Fry, N. L.; Martinez, J. L.; Mascharak, P. K. Syntheses, Structures and Properties of New Manganese Carbonyls as Photoactive CO-Releasing Molecules: Design Strategies That Lead to CO Photolability in the Visible Region. *Inorg. Chem.* **2012**, *51*, 11930–11940.

(18) Gonzalez, M. A.; Carrington, S. J.; Chakraborty, I.; Olmstead, M. M.; Mascharak, P. K. Photoactivity of Mono- and Dicarbonyl Complexes of Ruthenium(II) Bearing an N,N,S-Donor Ligand: Role of Ancillary Ligands on the Capacity of CO Photorelease. *Inorg. Chem.* **2013**, *52*, 11320–11331.

(19) Carrington, S. J.; Chakraborty, I.; Alvarado, J. R.; Mascharak, P. K. Differences in the CO Photolability of cis- and trans-[RuCl₂(azpy)-(CO)₂] Complexes: Effect of Metal-to-Ligand Back-Bonding. *Inorg. Chim. Acta* **2013**, *407*, 121–125.

(20) Haukka, M.; Kiviaho, J.; Ahlgrh, M.; Pakkanen, T. A. Studies on Catalytically Active Ruthenium Carbonyl Bipyridine Systems. Synthesis and Structural Characterization of [Ru(bpy)(CO)₂Cl₂], [Ru(bpy)(CO)₂Cl(C(O)OCH₃)], [Ru(bpy)(CO)₂Cl₂] and [Ru(bpy)(CO)₂ClH] (bpy = 2,2'-Bipyridine). *Organometallics* **1995**, *14*, 825–833.

(21) Pierrri, A. E.; Pallaoro, A.; Wu, G.; Ford, P. C. A Luminescent and Biocompatible PhotoCORM. *J. Am. Chem. Soc.* **2012**, *134*, 18197–18200.

(22) Carrington, S. J.; Chakraborty, I.; Mascharak, P. K. Rapid CO Release From a Mn(I) Carbonyl Complex Derived from Azopyridine upon Exposure to Visible Light and Its Phototoxicity toward Malignant Cells. *Chem. Commun.* **2013**, *49*, 11254–11256.

(23) Chakraborty, I.; Carrington, S. J.; Mascharak, P. K. Photo-delivery of CO by Designed photoCORMs: Correlation between Absorption in the Visible Region and Metal-CO Bond Labilization in Carbonyl Complexes. *ChemMedChem* **2014**, *9*, 1266–1274.

(24) Daniel, C.; Guillaumont, D.; Ribbing, C.; Minaev, B. Spin-Orbit Coupling Effects on the Metal-Hydrogen Bond Homolysis of $M(H)(CO)_3(H-DAB)$ ($M = Mn, Re$; H-DAB = 1,4-Diaza-1, 3-butadiene). *J. Phys. Chem. A* **1999**, *103*, 5766–5772.

(25) Vogler, A.; Kunkely, H. Excited State Properties of Organometallics Compounds of Rhenium in High and Low Oxidation States. *Coord. Chem. Rev.* **2000**, *200–202*, 991–1008.

(26) Sato, S.; Sekine, A.; Ohashi, Y.; Ishitani, O.; Blanco-Rodriguez, A. M.; Vlcek, A., Jr; Unno, T.; Koike, K. Photochemical Ligand Substitution Reactions of *fac*-[Re(bpy)(CO)₃Cl] and Derivatives. *Inorg. Chem.* **2007**, *46*, 3531–3540.

(27) Sato, S.; Matubara, Y.; Koike, K.; Falkenström, M.; Katayama, T.; Ishibashi, Y.; Miyasaka, H.; Taniguchi, S.; Chosrowjan, H.; Mataga, N.; Fukazawa, N.; Koshihara, S.; Onda, K.; Ishitani, O. Photochemistry of *fac*-[Re(bpy)(CO)₃Cl]. *Chem.—Eur. J.* **2012**, *18*, 15722–15734.

(28) Gonzales, M. A.; Han, H.; Moyes, A.; Radinos, A.; Hobbs, A. J.; Coombs, N.; Oliver, S. R. J.; Mascharak, P. K. Light-triggered Carbon Monoxide Delivery with Al-MCM-41-based Nanoparticles Bearing a Designed Manganese Carbonyl Complex. *J. Mater. Chem. B* **2014**, *2*, 2107–2113.

(29) Dördelman, G.; Pfeiffer, H.; Birkner, A.; Schatzschneider, U. Silicium Dioxide Nanoparticles as Carriers for Photoactivatable CO-Releasing Molecules (PhotoCORMs). *Inorg. Chem.* **2011**, *50*, 4362–4367.

(30) Pfeiffer, H.; Rojas, A.; Niesel, J.; Schatzschneider, U. Sonogashira and “Click” Reactions for the N-terminal and Side Chain Functionalization of Peptides with [Mn(CO)₃(tpm)]⁺ Based CO Releasing Molecules (tpm = tris(pyrazolyl)methane). *Dalton Trans.* **2009**, *22*, 4292–4298.